Proton Transfers in Hydrogen-Bonded Systems. Cationic Oligomers of Water

Steve Scheiner

Contribution from the Department of Chemistry and Biochemistry, Southern Illinois University, Carbondale, Illinois 62901. *Received May 21, 1980*

Abstract: Ab initio molecular orbital methods are used to calculate potential energy surfaces for proton transfers between water molecules in the linear hydrogen-bonded systems $H^+(H_2O)_n$, n = 2, 3, 4, and 5. The split valence-shell 4-31G basis set used is shown to provide results in excellent agreement with more sophisticated treatments which include correlation energy contributions. Geometry optimizations and inclusion of two additional water molecules have little effect upon the energy barriers to proton transfer in $H^+(H_2O)_2$. Linear and angular deformations of the hydrogen bond increase proton-transfer barriers in a nonlinear fashion. Predictive power of group charges and overlap populations are demonstrated as they correlate quite well with calculated proton-transfer barriers. Potentials calculated for $H^+(H_2O)_3$ are found to be subject to substantial end effects while the $H^+(H_2O)_5$ system is more representative of the situation in long hydrogen-bonded chains. The barriers to single- and double-proton transfers in the pentamer are approximately the same as those for single transfer in the dimer and tetramer. These results are discussed with particular regard to a proposed model of proton transport through biomembranes.

Introduction

Proton transfers are an important component in a wide array of chemical and biological processes[1] including photosynthesis,[2] mitochondrial oxidative phosphorylation,[3] bacterial metabolism,[4] and vision.[5] Evidence has accumulated that a common feature of the latter phenomena is transport of protons through a biomembrane. Biological membranes consist basically of a lipid bilayer with an extremely hydrophobic interior. It is therefore unlikely that the electrically charged protons move directly through the lipid interior. There are however "integral" or transmembrane protein molecules located within membranes that extend completely from the inside surface to the outside of the membrane.[6] These proteins, which contain hydrophilic as well as hydrophobic domains, offer a less hostile pathway for proton migration. Bacteriorhodopsin, for example, is thought to serve as an active proton conduit through the purple membrane of Halobacterium halobium.[4]

The large numbers of hydrogen bonds within protein molecules may offer an extremely efficient means of proton transport. This mechanism, originally suggested by Eigen[7] and Onsager[8] and further elaborated by Nagle and Morowitz,[9] presupposes the existence within the protein of a hydrogen bond chain of the general type OH··OH··OH··OH··OH··. Although the hydrogen bonding groups are represented here by hydroxyls which occur in the side chains of serine and in waters of hydration, it is emphasized that this is by no means a requirement. Various other hydrogen-bonding moieties of proteins might also participate in the chain. Hydrogen-bonded chains of this sort occur in murein lipoprotein,[10] bacteriorhodopsin,[4c,f] carbohydrates,[11] and the solid states of water,[7,8] alcohols,[12] imidazole,[13] and various other organic and inorganic materials,[14] as well as in liposomes.[15] An important step in the proton-transport process involves first the association of a proton with the leftmost residue of the chain. This initiates a series of transfers of protons from one residue to the next, with the rightmost proton being finally ejected from the chain.

Several recent theoretical treatments[16] have attempted to analyze the kinetics of this proton-transport mechanism. These procedures divide the entire process into individual steps, each of which consists of the hopping of a single proton from one residue to the next. Successful analysis is therefore contingent upon quantitative estimates of the energetics of each proton transfer. It is at this point that quantum chemical calculations can make a valuable contribution. Methods developed during the previous two decades are capable of providing accurate potential energy surfaces for processes such as proton transfers. It is therefore to this task that we turn our attention in this paper.

The calculations described below deal with proton transfers between hydroxyl groups and are therefore applicable to links in the chain consisting of serine, threonine, tyrosine, or waters of hydration. All links were modeled here by water molecules to facilitate the calculations. The work thus relates directly to water,

(1) Caldin, E.; Gold, V., Eds. "Proton Transfer Reactions"; Wiley: New York, 1975; and references contained therein.
(2) (a) Sauer, K. *Acc. Chem. Res.* **1978**, *11*, 257-264. (b) Mitchell, P. *Nature (London)* **1961**, *191*, 144-148; *Science (Washington, D.C.)* **1979**, *206*, 1148-1159; *Ann. Rev. Biochem.* **1977**, *46*, 996-1005. (c) Jagendorf, A. T. In "Bioenergetics of Photosynthesis"; Govindjee, Ed.; Academic Press: New York, **1975**; pp 413-492.
(3) (a) Reenstra, W. W.; Patel, L.; Rottenberg, H.; Kaback, H. R. *Biochemistry* **1980**, *19*, 1-9. (b) Pozzan, T.; DiVirgilio, F.; Bragadin, M.; Miconi, V.; Azzone, G. F. *Proc. Natl. Acad. Sci. U.S.A.* **1979**, *76*, 2123-2127. (c) Cohen, S. M.; Ogawa, S.; Rottenberg, H.; Glynn, P.; Yamane, T.; Brown, T. R.; Shulman, R. G.; Williamson, J. R. *Nature (London)* **1978**, *273*, 554-556.
(4) (a) Lewis, A.; Marcus, M. A.; Ehrenberg, B.; Crespi, H. *Proc. Natl. Acad. Sci. U.S.A.* **1978**, *75*, 4642-4646. (b) Henderson, R. *Ann. Rev. Biophys. Bioeng.* **1977**, *6*, 87-109. (c) Ovchinnikov, Yu. A.; Abdulaev, N. G.; Feigina, M. Yu.; Kiselev, A. V.; Lobanov, N. A. *FEBS Lett.* **1979**, *100*, 219-224. (d) Stoeckenius, W. *Sci. Am.* **1976**, *234*, No. 6, 38-46. (e) Nagle, J. F.; Mille, M. submitted for publication in *Biochim. Biophys. Acta*. (f) Engelman, D. M.; Henderson, R.; McLachlan, A. D.; Wallace, B. A. *Proc. Natl. Acad. Sci. U.S.A.* **1980**, *77*, 2023-2027.
(5) (a) Honig, B.; Ebrey, T.; Callender, R. H.; Dinur, U.; Ottolenghi, M. *Proc. Natl. Acad. Sci. U.S.A.* **1979**, *76*, 2503-2507. (b) Warshel, A. *Ibid.* **1978**, *75*, 2558-2562. (c) Peters, K.; Applebury, M. L.; Rentzepis, P. M. *Ibid.* **1977**, *74*, 3119-3123.
(6) (a) Bretscher, M. S. *Science (Washington, D.C.)* **1973**, *181*, 622-629. (b) Singer, S. J.; Nicolson, G. L. *Ibid.* **1972**, *175*, 720-731.
(7) (a) Eigen, M.; DeMaeyer, L. *Proc. R. Soc. London, Ser. A* **1958**, *247*, 505-533. (b) Eigen, M., *Angew. Chem., Int. Ed. Engl.* **1964**, *3*, 1-19.
(8) (a) Onsager, L. *Science (Washington, D.C.)* **1969**, *166*, 1359-1364; *Ibid.* **1967**, *156*, 541. (b) Chen, M. S.; Onsager, L.; Bonner, J.; Nagle, J. *J. Chem. Phys.* **1974**, *60*, 405-419.
(9) Nagle, J. F.; Morowitz, H. J. *Proc. Natl. Acad. Sci. U.S.A.* **1978**, *75*, 298-302.
(10) Dunker, A. K.; Marvin, D. A. *J. Theor. Biol.* **1978**, *72*, 9-16.
(11) Jeffrey, G. A.; Takagi, S. *Acc. Chem. Res.* **1978**, *11*, 264-270.
(12) Pauling, L. In "The Nature of the Chemical Bond"; Cornell University Press: Ithaca, N.Y., 1960; pp 473-475.
(13) Kawada, A.; McGhie, A. R.; Labes, M. M. *J. Chem. Phys.* **1970**, *52*, 3121-3125.
(14) (a) Negram, T. J.; Glass, A. M.; Brickencamp, C. S.; Rosenstein, R. D.; Osterheld, R. K.; Susott, R. *Ferroelectrics* **1974**, *6*, 179-182. (b) Schmidt, V. H.; Drumheller, J. E.; Howell, F. L. *Phys. Rev. B* **1971**, *4*, 4582-4597. (c) Glasser, L. *Chem. Rev.* **1975**, *75*, 21-65.
(15) Nichols, J. W.; Deamer, D. W. *Proc. Natl. Acad. Sci. U.S.A.* **1980**, *77*, 2038-2042.
(16) (a) Knapp, E.-W.; Schulten, K.; Schulten, Z. *Chem. Phys.* **1980**, *46*, 215-229. (b) Del Castillo, L. F.; Mason, E. A.; Viehland, L. A. *Biophys. Chem.* **1979**, *9*, 111-120. (c) Läuger, P. *Biochim. Biophys. Acta* **1979**, *552*, 143-161 (d) Fang, J. K.; Godzik, K.; Hofacker, G. L. *Ber. Bunsenges. Phys. Chem.* **1973**, *77*, 980-990. (e) Nagle, J. F.; Mille, M.; Morowitz, H. J. *J. Chem. Phys.* **1980**, *72*, 3959-3971.

0002-7863/81/1503-315$01.00/0

but, as explicit inclusion of the full amino acid residues would not be expected to produce large changes in the calculated potentials, the results may be considered as representative of the hydroxyl-containing residues as well.

Proton transfers between water molecules have been investigated previously by ab initio[17-26] and semiempirical methods.[26-30] These studies have, however, been concerned principally with the optimal orientations of the water molecules; i.e., the proton transfer has been considered as taking place when the two oxygen atoms are located at an optimal separation of ca. 2.4 Å. This short hydrogen bond distance is however very seldom found in proteins due to a large number of structural constraints. For this reason, the present calculations determine systematically the energetics of proton transfer with longer interresidue distances. Also, for the first time, the effects of bending as well as stretching of the hydrogen bond are calculated. A further question considered here concerns the cooperativity of proton transfers; e.g., is it energetically favorable for several proton transfers to take place simultaneously.

Methods and Results

Ab initio molecular orbital calculations were performed by using the GAUSSIAN 70 program developed by Pople and co-workers.[31] The split valence-shell 4-31G basis set[32] was employed to calculate the energies and wave functions of linear hydrogen-bonded chains of the type $H^+(H_2O)_n$, n = 2, 3, 4, and 5. The latter basis set has been found previously to provide reliable results for similar systems[17,18] and is shown below to be in excellent agreement with much more elaborate quantum mechanical techniques. The wave functions were analyzed by using the standard Mulliken procedure for obtaining atomic charges and overlap populations.[33]

The geometry of $(H_5O_2)^+$ has been optimized previously by Newton and Ehrenson[18] by using the 4-31G basis set. Their structure is of D_{2d} symmetry with the planes of the two water molecules staggered by 90° with respect to one another. The interoxygen distance, R, is 2.36 Å, and the central hydrogen is located midway between the two oxygen atoms.

Potential energy curves for proton transfer between the two water molecules were obtained by calculating the energy of the system as a function of the distance, r, between the central hydrogen and one of the oxygen atoms. All nuclei with the exception of the central proton were held stationary during the transfer. The potentials for various values of the interoxygen separation, R, are presented as dashed curves in Figure 1. (Each curve represents only the left half of the full transfer. Due to the symmetry of the system, the right half of each curve is the mirror image of the left.)

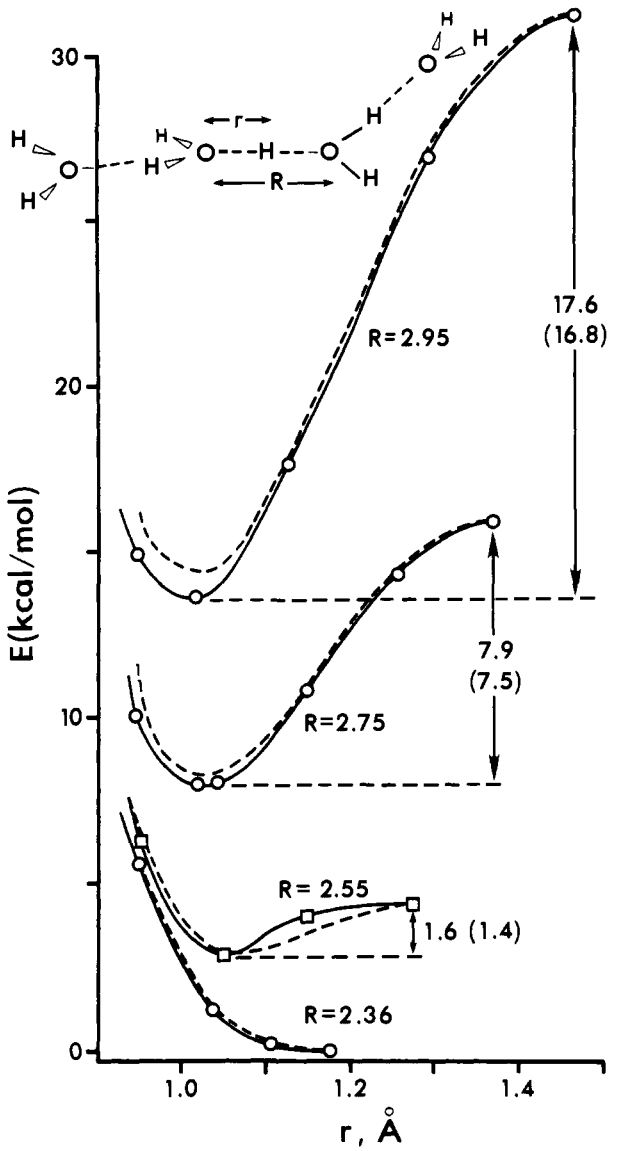

Figure 1. Proton-transfer potentials for $(H_5O_2)^+$ (dashed curves) and $(H_9O_4)^+$ (solid curves). Energy barriers shown in parentheses refer to dimers. Tetramer energies are relative to the configuration R = 2.36 Å and r = 1.18 Å. The dimer curves are superposed on tetramer curves such that midpoint energies coincide. The terminal water molecules in the tetramer have internal geometry r(OH) = 0.95 Å and θ(HOH) = 112° while for the central waters, r(OH) = 1.00 Å and θ(HOH) = 120°. All hydrogen bonds are linear; i.e., θ(OHO) = 180°. Successive water molecules are staggered with respect to one another. The water molecules in the dimer have internal geometry r(OH) = 0.95 Å and θ(HOH) = 115°.

It may be noted that for small values of the interoxygen distance (e.g., the optimized R = 2.36 Å) the potential contains a single minimum. The preferred position of the central proton is thus midway between the two oxygen atoms when the two water molecules are relatively close together. For larger values of R, the potential acquires double-well character. The two equivalent energy minima each correspond to a configuration in which the central proton is associated with one water molecule or the other. This proton is midway between the two oxygens in the transition state to proton transfer defined here as the top of the energy barrier separating the two minima. The transformation from single- to double-well character occurs at approximately R = 2.4 Å, and one may note the rapid increase in the height of the energy barrier as the two water molecules are further separated. A second effect

(17) Newton, M. D. *J. Chem. Phys.* **1978**, *67*, 5535-5546.
(18) Newton, M. D.; Ehrenson, S. *J. Am. Chem. Soc.* **1971**, *93*, 4971-4990.
(19) Janoschek, R.; Weidemann, E. G.; Zundel, G. *J. Chem. Soc., Faraday Trans. 2* **1973**, *69*, 505-520.
(20) Janoschek, R.; Weidemann, E. G.; Pfeiffer, H.; Zundel, G. *J. Am. Chem. Soc.* **1972**, *94*, 2387-2396.
(21) Kollman, P. A.; Allen, L. C. *J. Am. Chem. Soc.* **1970**, *92*, 6101-6107.
(22) Kraemer, W. P.; Diercksen, G. H. F. *Chem. Phys. Lett.* **1970**, *5*, 463-465.
(23) Meyer, W.; Jakubetz, W.; Schuster, P. *Chem. Phys. Lett.* **1973**, *21*, 97-102.
(24) Alagona, G.; Cimiraglia, R.; Lamanna, V. *Theor. Chim. Acta* **1973**, *29*, 93-96.
(25) Delpuech, J.-J.; Serratrice, G.; Strich, A.; Veillard, A. *Mol. Phys.* **1975**, *29*, 849-871.
(26) Schuster, P.; Jakubetz, W.; Beier, G.; Meyer, W.; Rode, B. M. In "Chemical and Biochemical Reactivity"; Bergmann, E. D., Pullman, B., Eds.; Academic Press: Jerusalem, 1974; pp 257-282.
(27) Janoschek, R. In "The Hydrogen Bond-Recent Developments in Theory and Experiments"; Schuster, P., Zundel, G., Sandorfy, C., Eds.; North-Holland Publishing Co.: Amsterdam, 1976; pp 167-216.
(28) Ingraham, L. L. *Biochim. Biophys. Acta* **1972**, *279*, 8-14.
(29) Gandour, R. D.; Maggiora, G. M.; Schowen, R. L. *J. Am. Chem. Soc.* **1974**, *92*, 6967-6979.
(30) Chojnacki, H. *Int. J. Quantum Chem.* **1979**, *16*, 299-309.
(31) Hehre, W. J.; Lathan, W. A.; Ditchfield, R.; Newton, M. D.; Pople, J. A. GAUSSIAN 70, Program No. 236, Quantum Chemistry Program Exchange, Indiana University, Bloomington, Ind., 1974.
(32) Ditchfield, R.; Hehre, W. J.; Pople, J. A. *J. Chem. Phys.* **1971**, *54*, 724-728.
(33) Mulliken, R. S. *J. Chem. Phys.* **1955**, *23*, 1833-1840.

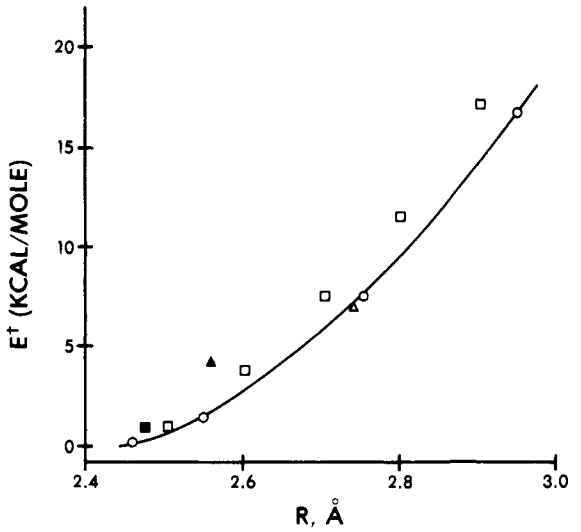

Figure 2. Calculated barriers to proton transfer in $(H_5O_2)^+$: ○, 4-31G; □, 46 basis functions;[20] ■, double-ζ;[21] ▲, [541/31];[22] △, [531/311] + CI.[23]

Table I. Barriers to Proton Transfer

	$E^\dagger$, kcal/mol			
R, Å	$(H_5O_2)^+$ rigid staggered	$(H_5O_2)^+$ optimized staggered	$(H_9O_4)^+$ rigid staggered	$(H_5O_2)^+$ rigid eclipsed
2.55	1.4	1.7	1.6	1.4
2.75	7.5	8.0	7.9	7.6
2.95	16.8	17.5	17.6	16.9

of the increase in R is the diminution of the equilibrium value of r, shrinking from 1.18 Å at R = 2.36 to 1.04 Å at R = 2.75 Å. As the two water molecules are pulled apart, the association of the central hydrogen with the nearer of the oxygen atoms thus becomes more pronounced.

It was thought necessary at this point to ascertain the reliability of the 4-31G method. There are available several ab initio proton-transfer potentials which have been obtained previously for $(H_5O_2)^+$ by using larger basis sets and including electron correlation effects.[20-23] The barrier heights obtained by the various procedures are presented in Figure 2 where the solid curve represents the 4-31G results calculated here. The figure indicates that at the Hartree–Fock level, basis sets larger than 4-31G yield higher barriers but that inclusion of electron correlation reduces these barriers. The net result is that 4-31G furnishes transfer barriers in excellent agreement with much more sophisticated theoretical treatments using large basis sets and configuration interaction. A second factor which may have some bearing on the proton-transfer potentials concerns the assumption of internally rigid water molecules. Some internal rearrangements within each molecule might be expected as the proton is being transferred. For a test of the effect of any rearrangements on the magnitudes of the barriers, full geometry optimizations were performed for each stage of the proton transfer, subject to C_{2v} symmetry restraints (D_{2d} for the midpoint). Comparison of the first two columns of Table I indicates that barriers calculated by using optimized geometries are only slightly greater than those obtained by using the rigid-molecule assumption. Therefore, all the potentials presented in this paper have been calculated using the latter approximation to reduce computational time requirements.

The two water molecules studied up until this point encompass only a small segment of the 20 or so links along the chain needed to span a biomembrane.[9] It is necessary therefore to examine systems composed of larger numbers of hydrogen-bonding groups. One additional water molecule was added to each end of the H_2O–H^+–OH_2 moiety to enlarge the system, forming the $(H_9O_4)^+$ configuration described in Figure 1. The tetramer structure has been previously optimized[18] and belongs to the C_2 point group.

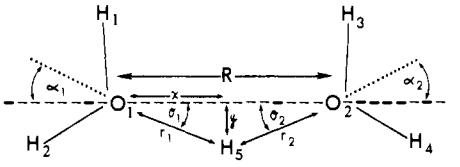

Figure 3. Hydrogen bond deformations in $(H_5O_2)^+$. α_1 and α_2 are both positive as shown. All atoms lie in a common plane.

The terminal water molecules were kept at a fixed distance (2.54 Å) from the central molecules and several values of R, the distance between the two central oxygen atoms, were chosen for study. For each value of R, the transferring proton was moved along the central interoxygen axis as the remainder of the system was held fixed. Proton-transfer potentials for the tetramer are shown as solid curves in Figure 1 where they may be compared with the analogous potentials for the dimer (dashed curves). The similarity of dimer and tetramer potentials is quite apparent. The tetramer barriers listed in the penultimate column of Table I are only slightly different from the dimer barriers. Further elongation of the chain to perhaps six or eight water units would not be expected to produce any substantial additional changes. It thus appears that the $(H_5O_2)^+$ dimer may serve as an excellent model for studying proton transfers in longer chains and that end effects are of little importance here.

It is of some interest to examine the electronic charge redistributions induced by the addition of the two terminal water molecules to the $(H_5O_2)^+$ species to form $(H_9O_4)^+$. Charges were assigned to atomic centers using a standard Mulliken population analysis.[33,34] The overall effect of the two added water molecules is to pull positive charge outward from the center of the system. The positive charge assigned to the central proton is reduced by some 30–40 millielectrons while the terminal waters acquire a combined positive charge of 126 millielectrons. As the central proton moves from its endpoint position near the left central water molecule ($H_2O(H_3O)^+H_2OH_2O$) to the midpoint ($H_2OH_2OH^+H_2OH_2O$), the total positive charge of the left terminal water decrease somewhat. However, this change is exactly counterbalanced by an increased positive charge on the right terminal water. The net result is that the combined charge of the two terminal water molecules remains quite constant during the course of the proton transfer. This constant charge is noted for all three values of R between 2.55 and 2.95 Å.

We now return our attention to the dimer species $(H_5O_2)^+$. The calculations described above have all been based on the previously optimized geometry[18] in which the two water molecules are staggered by 90° with respect to one another. In order to ascertain the sensitivity of the results to rotations about the interoxygen axis, proton-transfer potentials were calculated for the eclipsed configuration in which all atoms lie in a common plane. Barriers obtained for this arrangement are listed in the last column of Table I where they may be compared with values calculated for the staggered conformations. It is clear from the data in the table that barrier heights of $(H_5O_2)^+$ are little affected by (a) geometry optimization, (b) addition of two terminal water molecules, or (c) rotation to the eclipsed configuration.

Hydrogen Bond Deformations. As pointed out in the Introduction, it is a major objective of this investigation to examine the effects of deformations of the hydrogen bond on the potentials for proton transfer. Angular deformations considered are represented by α_1 and α_2 which are defined as the angles made by the respective HOH bisectors of the two water molecules with the OO internuclear axis (see Figure 3). It should be noted that when $\alpha_1 = \alpha_2 = 0°$, the configuration is identical with the eclipsed geometry described above. Proton-transfer potentials were calculated for each set of values (R, α_1, α_2) by translating the central

(34) It has been pointed out previously[18] that double-ζ-type basis sets without polarization functions (e.g., 4-31G) have a marked tendency toward very low electron densities on H atoms. More chemically meaningful results may be achieved by consideration of overall charges of several atoms considered as a group or of *changes* in electron densities of individual atoms.

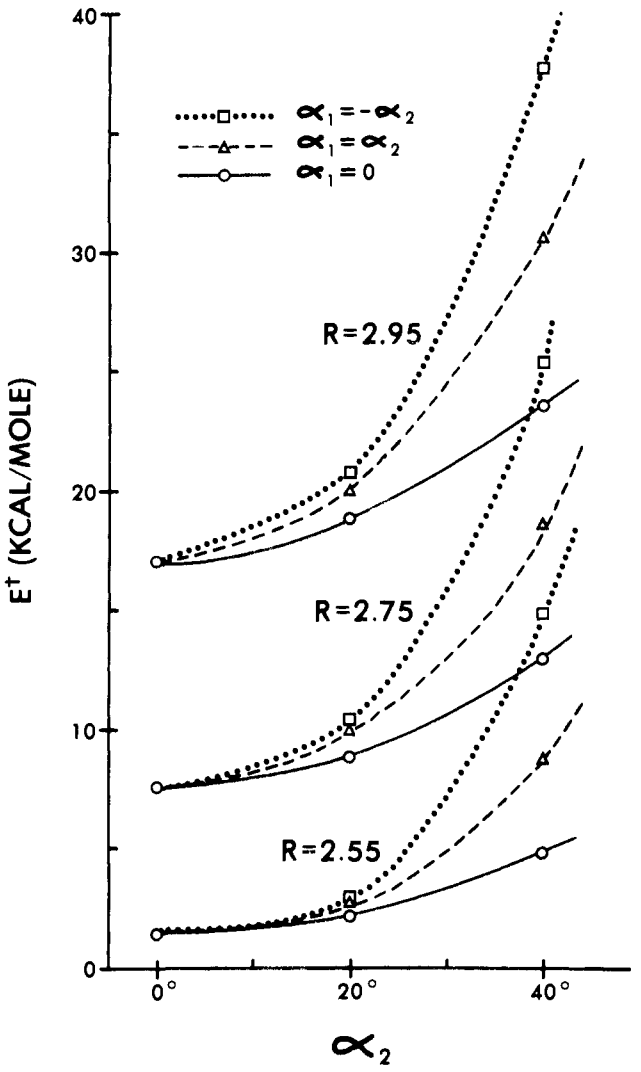

Figure 4. Proton-transfer barriers in distorted configurations of $(H_5O_2)^+$.

proton H_5 a given distance x along the interoxygen axis and optimizing its vertical displacement y from this line. Motions of the proton out of the molecular plane resulted in increased energy for all configurations examined.

For each of three values of R, three modes of angular deformation were examined. First, one water molecule was held in its optimum orientation ($\alpha_1 = 0°$) and the other rotated. This mode is represented by the solid curves in Figure 4. In a second mode, denoted by dashed lines, both waters were rotated by equal amounts and in the same direction ($\alpha_1 = \alpha_2$); i.e., the oxygen lone pairs of both waters point below the interoxygen axis (see Figure 3). The third mode is similar except that the waters were rotated by equal amounts in *opposite* directions ($\alpha_1 = -\alpha_2$). The latter mode is represented by dotted curves.

Figure 4 shows that the barrier to proton transfer becomes more pronounced with increasing angular as well as linear deformations of the hydrogen bond. The barrier height enlargement is fairly small for deformations under 20° but becomes quite severe as the distortion increases further. In addition, the magnitude of the barrier is more sensitive to angular deformations for larger values of R. The mode of distortion which produces the highest barriers is that in which the two waters are rotated in opposite directions ($\alpha_1 = -\alpha_2$).

Analyses of the electronic wave functions reveal some interesting relationships between the energetics and electron density distributions. For each geometry, as defined by the values (R, α_1, α_2), we consider first the initial configuration $(H_3O)^+H_2O$ in which the central proton is associated with water molecule a. Q is defined as the total electron density assigned to the water molecule b to which the proton is being transferred ($H_3O_2H_4$ in Figure 3). This

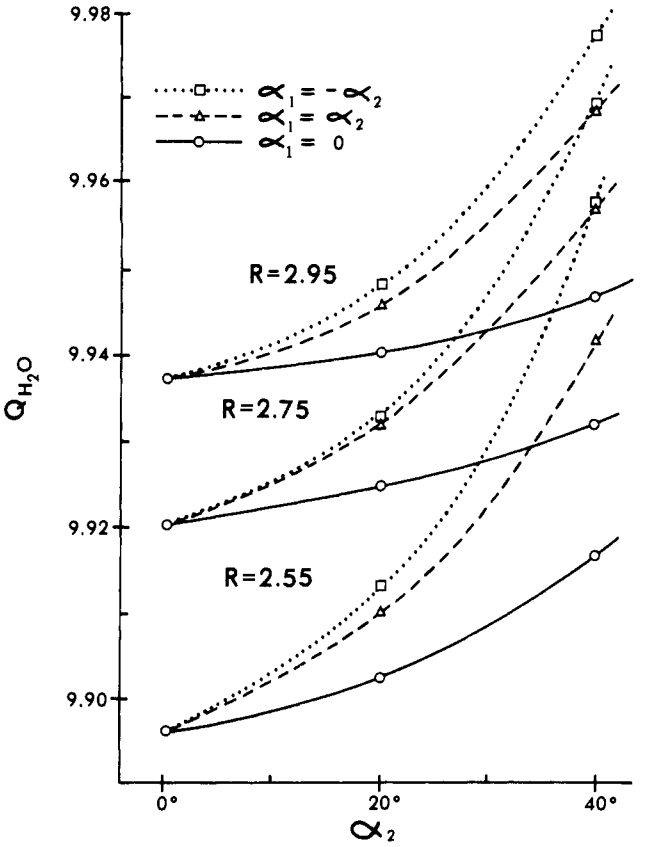

Figure 5. Total electron density of proton acceptor H_2O in the initial configuration $(H_3O)^+H_2O$. The total charge of H_2O associated with density Q is equal to $10 - Q$.

density is shown in Figure 5 as a function of various hydrogen bond deformations. It may be noted first that as water molecule b is pulled away to greater distances from H_3O^+, i.e., as R is increased, the electron density on H_2O rises toward its value of 10 at infinite separation. Angular deformations of the hydrogen bond also result in greater electron density on this water. The latter trends are not unexpected as this water molecule is acting as an electron donor. Distortions of the hydrogen bond would be expected to reduce the charge being transferred to H_3O^+ and hence increase the density remaining on H_2O. However, the close similarity between the electron densities presented in Figure 5 and the energy barriers depicted in Figure 4 is particularly striking. The charges assigned to the central hydrogen, H_5, in the various initial configurations follow a similar pattern with smaller deformations leading to a depletion of the proton's electron density.

The overlap populations, too, show a strong correlation with proton transfer barriers. We consider again the initial configurations $(H_3O)^+H_2O$ in which the central hydrogen is strongly bound to O_1 and only weakly bound to the electron donor O_2 (O_1–H···O_2). A plot of the overlap population between the central hydrogen and either O_1 or O_2 vs. bond deformations bears very strong resemblance to Figures 4 and 5. If we consider the overlap population as an indicator of "bond strength", we find that hydrogen bond deformations lead to a weakening of the H···O_2 interaction and concomitant strengthening of the O_1–H bond.

The group charges and overlap populations obtained from a calculation of only the initial $(H_3O)^+H_2O$ configuration may thus have great usefulness in predicting energetics of the proton-transfer potentials. Least-squares linear regression analyses result in the following relationships between the barrier $E^\dagger$, the electron density Q of H_2O, and the overlap populations P_{O_1H} and P_{HO_2}.

$$E^\dagger = 401Q_{H_2O} - 3970$$

$$E^\dagger = 324P_{O_1H} - 43.3$$

$$E^\dagger = -425P_{HO_2} + 40.6$$

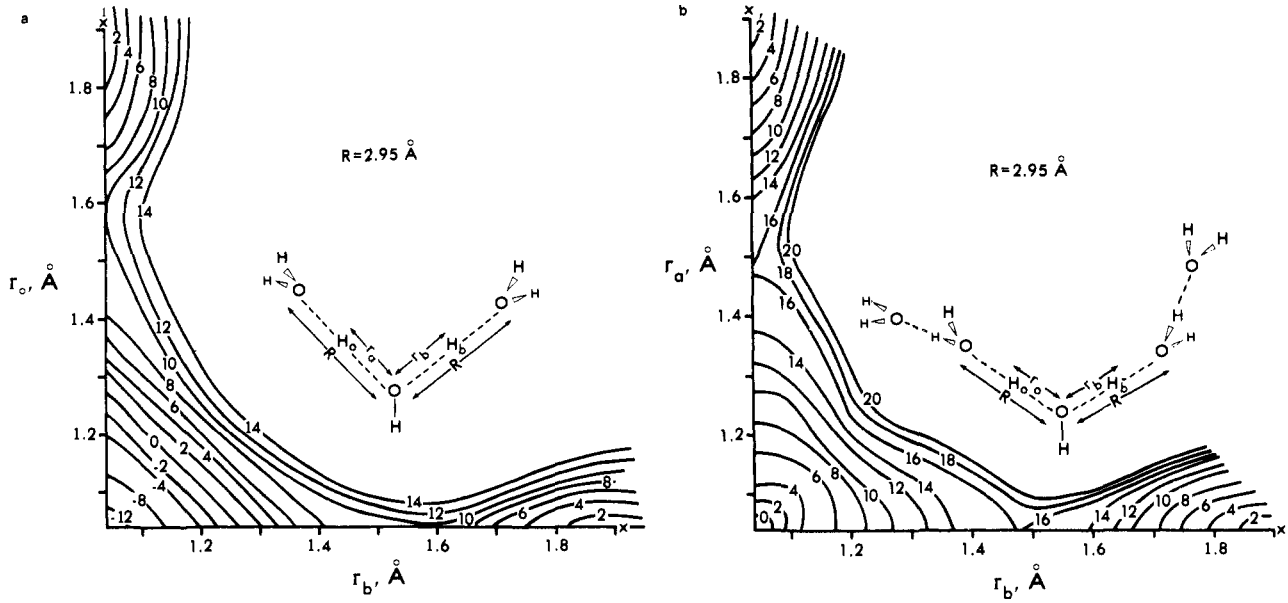

Figure 6. Isoenergy (kcal/mol) contour maps calculated for double-proton transfers in (a) $(H_7O_3)^+$ and (b) $(H_{11}O_5)^+$. All hydrogen bonds are linear; i.e., $\theta(OHO) = 180°$. Water molecules other than the central one have internal geometry $r(OH) = 0.95$ Å and $\theta(HOH) = 112°$. The angles $\theta(HOH)$ in the central (planar) water are 120°. All adjacent water molecules are staggered; i.e., $\phi(HOOH) = 90°$. The trimer is of C_{2v} symmetry. The terminal hydrogen bonds in the pentamer are such that $r(OO) = 2.54$ Å.

The correlation coefficients for these three relationships are 0.92, 0.90, and 0.92, respectively.

For each geometry (R, α_1, α_2), a comparison of charge distributions in the initial and transition-state configurations revealed that the central proton suffers a depletion of electron density upon being transferred from one water molecule to a position approximately midway between the two waters. The magnitude of this charge loss ranges between 20 and 80 millielectrons. The electron donor water molecule b undergoes an analogous density decrease of some 60–150 millielectrons. In either case, the larger charge transfers are associated with greater deformations of the hydrogen bond. As the charges of the individual species in the transition-state configurations are relatively insensitive to geometrical distortions, varying by at most 30 millielectrons, the larger charge redistributions occurring upon half proton transfer in the deformed hydrogen bonds are due chiefly to the electron density rearrangements in the initial configurations.

Multiple Proton Transfers. The transport of a proton through the entire span of the biomembrane requires on the order of 20 hops of protons from one residue to the next in the hydrogen-bonding chain. Up until this point we have been treating single jumps of one proton. However, it is certainly feasible that the entire process may be greatly facilitated by concerted transfers wherein two or more protons are transferred simultaneously. Drawing an analogy with a fire bucket brigade, simultaneous proton transfer corresponds to a member of the chain passing off a bucket to the next person in line at the same time as receiving another bucket from the previous member.

For a study of this concerted mechanism, the cationic water trimer $(H_7O_3)^+$ pictured in Figure 6a was used as a model system. The geometry of the linear trimer was taken initially from a previous 4-31G optimization[18] as described in the figure caption. The interoxygen distances, R, were set to 2.95 Å, and the energy was calculated as a function of the distances r_a and r_b of the two protons H_a and H_b from the central oxygen atom. We take the zero of energy to be that of the initial configuration $(H_3O)^+(H_2O)(H_2O)$ in which the extra proton is associated with a terminal water molecule. The position of this configuration is marked by the × located in the upper left corner of the figure at $r_a = 1.91$ Å and $r_b = 1.04$ Å. A single proton transfer is considered as the motion of the excess proton H_a from the leftmost to the central water. The resulting configuration $(H_2O)(H_3O)^+(H_2O)$ corresponds to the lower left corner of the figure. A full double transfer which places an excess proton (H_b) on the rightmost water leads to the configuration $(H_2O)(H_2O)(H_3O)^+$ denoted by the × in the lower right corner. The calculated results for various values of r_a and r_b are shown as isoenergy contours in Figure 6a. The symmetry of the contour lines about the diagonal ($r_a = r_b$) is a consequence of the C_{2v} symmetry of the molecular geometry.

Let us examine the energetics of proton transfer by beginning with the initial configuration $(H_3O)^+(H_2O)(H_2O)$ in the upper left corner. The optimal path from this point is vertically downward, i.e., r_b constant. As H_a begins to move from the left to the central oxygen, any accompanying motion of H_b from the central to right oxygen results in a rather steep increase in energy. When r_a has decreased to ca. 1.6 Å, the energy has increased by 10 kcal/mol but the single transfer to $(H_2O)(H_3O)^+(H_2O)$ may then be completed with steadily decreasing energy. From the same point ($r_a = 1.6$ Å, $r_b = 1.04$ Å), further decrease in r_a may alternatively be coupled to increases in r_b, thus effecting the double transfer to $(H_2O)(H_2O)(H_3O)^+$, also without further increase in energy. The point of highest energy along either path, which is defined here as the transition state, corresponds to a configuration in which H_a has been partially transferred but H_b has not moved from its position in the initial configuration. The activation energy of 10 kcal/mol found here is substantially less than $E^\dagger$ calculated for the dimer with R = 2.95 Å (17 kcal/mol). It would thus appear at first sight that in some fashion the transfer of a proton is made more facile by the incipient transfer of a second proton.

This conclusion would, however, be incorrect as a more detailed analysis reveals that end effects are chiefly responsible for the lower activation energy in the trimer. It may be noted, for example, that the lowest energy configuration, occurring at $r_a = r_b = 1.04$ Å, is $(H_2O)(H_3O)^+(H_2O)$ in which the central water molecule bears the extra proton. This structure is calculated to be 14 kcal/mol more stable than $(H_3O)^+(H_2O)(H_2O)$ where the positive charge is located on a terminal water. The extra stabilization of the former structure may be explained by the fact that the central water is involved in two hydrogen bonds and a terminal water in only one. The central water may therefore accommodate the extra charge better than a terminal water, and the corresponding configuration is hence more stable. The Mulliken group charge of the $(H_3O)^+$ unit is calculated to be +0.88 in $(H_2O)(H_3O)^+(H_2O)$ and +0.92 in $(H_3O)^+(H_2O)(H_2O)$. By cutting off the chain at only 3 units, we are therefore inducing what may perhaps loosely be described as an "electric field" which tends to draw the positive charge toward the center of the system.

The end effects may be greatly diminished by adding an additional water molecule to both ends of the trimer, forming the

$(H_{11}O_5)^+$ pentamer system illustrated in Figure 6b. The two additional waters were placed as shown at a distance of 2.54 Å from the oxygen atoms of the neighboring waters, and the geometry of the remainder of the system was left unaltered from that shown in Figure 6a. Once again, the energy was calculated as a function of the positions of the two central protons H_a and H_b while all other nuclei were held stationary. The isoenergy contours for the pentamer, shown in Figure 6b, exhibit many of the same qualitative features as the potential energy surface for the trimer. For example, the transition states for both systems occur when one proton has been partially transferred and the other remains on the central water. The transition state for the pentamer is found to occur slightly later (r_a = 1.5 Å) than for the trimer (1.6 Å). Other quantitative changes include an increase in the activation energy from 10 to 16 kcal/mol on going from the trimer to the pentamer. Also, the $(H_2O)(H_3O)^+(H_2O)$ configuration is only 2 kcal/mol more stable than $(H_3O)^+(H_2O)(H_2O)$ in the pentamer whereas the analogous quantity was 14 kcal/mol in the trimer.

All of the above changes may in fact be attributed to the attenuation of end effects in the pentamer as compared to the trimer. As mentioned previously, association of a third proton with a terminal water represents a rather unfavorable situation for the trimer as only one hydrogen bond is available to help alleviate the charge. In the pentamer, however, the same molecule is involved in two hydrogen bonds as is the central water. Consequently, the configuration in which the charge is associated with the central water is approximately equal in energy to that in which the extra proton is on an adjacent molecule. This near equality indicates that end effects have been greatly reduced and that the pentamer presents us with a realistic picture of the situation in long hydrogen bond chains. The activation energy of 16 kcal/mol found for the pentamer is approximately the same as that calculated for the dimer and tetramer with the same value of R (see Figure 1). This fact again points to the reliability of calculations involving only the dimer in obtaining activation energies for proton transfers in larger systems. Comparisons of the potential surfaces of $H^+(H_2O)_n$, n = 2, 3, 4, and 5 for R = 2.75 and R = 2.55, all lead to the same conclusions as drawn here for R = 2.95.

The transition state in the pentamer involves the partial transfer of only one proton. From the transition-state configuration, the energy of the system decreases monotonically toward either the single- or double-proton transferred products. It therefore appears that once enough energy has been harnessed to achieve the transition state which involves partial transfer of one proton, the transfer of a second proton may be coupled to the completion of the transfer with no additional expense in energy. This fact is suggestive that perhaps in the longer hydrogen bond chains, a large number of protons may be transferred simultaneously at no more cost in energy than only a single transfer.

Acknowledgment. I wish to thank Professor John F. Nagle for making available results prior to publication and the Southern Illinois University Academic Computing Center for a grant of computer time. This work was supported in part by the Research Corp.

Photoredox Reactions in Functional Micellar Assemblies. Use of Amphiphilic Redox Relays To Achieve Light Energy Conversion and Charge Separation

Pierre-Alain Brugger, Pierre P. Infelta, André M. Braun, and Michael Grätzel*

Contribution from the Institut de Chimie Physique, Ecole Polytechnique Fédérale, 1015 Lausanne, Switzerland. *Received April 7, 1980*

Abstract: The photoreduction of a homologous series of amphiphilic viologens (C_nMV^{2+}) using $Ru(bpy)_3^{2+}$ and zinc tetrakis(*N*-methylpyridyl)porphyrin ($ZnTMPyP^{4+}$) as sensitizers (S) was studied in water and aqueous solution containing cationic micelles.

$$S + C_nMV^{2+} \underset{\Delta}{\overset{h\nu}{\rightleftharpoons}} S^+ + C_nMV^+$$

Here, C_nMV^{2+} stands for *N*-alkyl-*N'*-methyl-4,4'-dipyridinium dichloride (alkyl = dodecyl ($C_{12}MV^{2+}$), tetradecyl ($C_{14}MV^{2+}$), hexadecyl ($C_{16}MV^{2+}$), and octadecyl ($C_{18}MV^{2+}$)). The forward electron transfer occurs with the viologen present in the aqueous phase. Upon reduction the relay acquires hydrophobic properties leading to rapid solubilization in the micelles. The subsequent thermal back-reaction is impaired by the positive surface potential of the aggregates. This decreases the rate constant for the electron back-transfer at least 500-fold. The stabilization and yield of redox products are optimal in a system containing $ZnTMPyP^{4+}$ as the sensitizer, $C_{14}MV^{2+}$ as a relay, and cetyltrimethylammonium chloride micelles. A kinetic model is presented to explain the effects observed, and implications for energy conversion systems are discussed.

Introduction

In the photoredox reaction

$$A + D \underset{\Delta}{\overset{h\nu}{\rightleftharpoons}} A^- + D^+ \quad (1)$$

light acts as an electron pump[1] promoting charge transfer from the donor (D) to the acceptor (A) under production of the high energy intermediates A^- and D^+. If the chemical potential of A^- and D^+ is to be utilized in subsequent fuel-generating processes, it is mandatory to prevent or retard the energy wasting back-reaction.[2] Molecular organizations such as micelles can serve this purpose since they possess charged microscopic interfaces which afford an electrostatic barrier to accomplish the charge

(1) Balzani, V.; Moggi, L.; Manfrin, M. F.; Bolletta, F.; Gleria, M. *Science (Washington D.C.)* **1975**, *189*, 852. (b) Calvin, M. *Photochem. Photobiol.* **1976**, *23*, 425. Porter, G.; Archer, M. D. *ISR, Interdiscip. Sci. Rev.* **1976**, *1*, 119. (d) Bolton, J. R., Ed. "Solar Power and Fuels"; Academic Press: New York, 1977. (e) Bolton, J. R. *Science (Washington, D.C.)* **1978**, *202*, 105. (f) Pioneering work on photoredox reactions in homogeneous sytems was carried out by Weller et al.; see, for example: Knibbe, H.; Rehm, D.; Weller, A. *Ber. Bunsenges. Phys. Chem.* **1969**, *73*, 839; Rehm, D.; Weller, A. *Ibid.* **1969**, *73*, 834. (g) For a recent review see also: Schumacher, E. *Chimia* **1978**, *32*, 193.

(2) For kinetic control of light-induced redox reaction by using: (a) BLM, cf.: Tien, H. T. *Top. Photosynth.* **1979**, *3*, 116-173. (b) Monolayers, cf.: Kuhn, H. *J. Photochem.* **1979**, *10*, 111. (c) Vesicles, cf.: Ford, W. E.; Otvos, J. W.; Calvin, M. *Proc. Natl. Acad. Sci. U.S.A.* **1979**, *76*, 3590. Ford, W. E.; Otvos, J. W.; Calvin, M. *Nature (London)* **1978**, *274*, 507. Calvin, M. *Int. J. Energy Res.* **1979**, *3*, 73. Infelta, P. P.; Fendler, J. H.; Grätzel, M. *J. Am. Chem. Soc.* **1980**, *102*, 1479.

0002-7863/81/1503-320$01.00/0